J. Anal. Appl. Pyrolysis 85 (2009) 399–407

Contents lists available at ScienceDirect

Journal of Analytical and Applied Pyrolysis

journal homepage: www.elsevier.com/locate/jaap

Structural properties of non-combustion-derived refractory organic matter which interfere with BC quantification

José María de la Rosa Arranz [a,c,*], Francisco J. González-Vila [a], Elisa López-Capel [b], David A.C. Manning [b], Heike Knicker [a,c], José Antonio González-Pérez [a]

[a] IRNAS, C.S.I.C, Avda. Reina Mercedes, 10, P.O. Box 1052, 41080 Sevilla, Spain
[b] School of Civil Engineering and Geosciences, University of Newcastle, Newcastle upon Tyne, NE1 7RU, UK
[c] Lehrstuhl für Bodenkunde, Technische Universität Munchen, D-85350 Freising-Weihenstephan, Germany

ARTICLE INFO

Article history:
Received 30 June 2008
Accepted 18 November 2008
Available online 27 November 2008

Keywords:
Refractory organic matter
Black carbon
Thermogravimetry
Analytical pyrolysis

ABSTRACT

Black carbon (BC), presenting the residue from incomplete combustion processes of fossil fuels and vegetation, has received special interest as a possible carbon sink in soils and sediments. In spite of this, there is still a need to develop accurate and comparable analytical protocols to determine the amount of BC stored in different environmental matrices and to characterise potentially interfering materials in the analysis of BC. Therefore in this study a melanoidin, a sample from the Green River Shale, a lignite and a bituminous coal were characterised by means of elemental analysis, thermogravimetry–differential scanning calorimetry (TG–DSC), pyrolysis coupled with gas chromatography–mass spectrometry (Py-GC/MS) and ^{13}C NMR spectroscopy. Thermal analysis (TG–DSC) indicated larger contributions of labile OM in the melanoidin and in the shale samples than in the lignite and the bituminous coal, although the coals showed an intense exothermal peak at temperatures higher than 550 °C. This behaviour is in agreement with high thermal recalcitrance of the latter and was also found in earlier studies of BC-rich material. Comparable to the latter, Py-GC/MS of the coals reveals considerable amounts of lignin-derived products. This and the similar thermal behaviour of both refractory materials aggravate their discrimination during BC-analysis. The pyrogram of the melanoidin reveals an important contribution of furanes and pyrane-like structures that derive from carbohydrates. NMR spectroscopy supports that those compounds are original constituents of the melanoidin rather than solely pyrolysis products. Considering that those compounds are typically formed during charring of N-containing biomass, their contribution to the BC structure should not be neglected if one seeks for a better understanding of BC structural properties. For the shale sample, both analytical pyrolysis and ^{13}C NMR spectroscopy confirm a high contribution of long alkyl-C chains. Due to their high hydrophobicity such structures can stand chemical oxidation and their presence in soil and sediment samples can obscure BC quantification by those methods. This study indicates that present approaches for BC-identification that are based on the assumption of BC being mostly a highly condensed polyaromatic network, have to be taken with caution and modified in accordance with a more heterogeneous composition of BC containing considerable fractions of only partly charred biopolymers.

1. Introduction

Black carbon (BC), soot, elemental carbon and charcoal are different terms used to describe a chemically heterogeneous, biologically refractory form of organic matter (ROM) remaining as residue from incomplete combustion processes. This particular organic material is ubiquitous and has been found in the atmosphere, ice, soils and sediments due to its widespread production, stability and inertness in the environment [1]. BC has received special interest in recent years as a possible carbon sink in soils and sediments. At present, there is not a single accepted method to detect and quantify BC forms, and therefore to provide the analytical data required for estimating BC contribution to terrestrial and sedimentary carbon pools, C fluxes and to the global carbon cycle.

BC is not a pure substance but rather a continuum of materials with different physicochemical properties and its isolation presents significant experimental constrains. In general, the cut-off between conventional organic carbon and BC in

* Corresponding author. Tel.: +34 954624711; fax: +34 954624007.
E-mail address: jmrosa@irnase.csic.es (J.M. de la Rosa Arranz).

Abbreviations: TG, thermogravimetry; DSC, differential scanning calorimetry; Py-GC/MS, pyrolysis coupled to gas chromatography–mass spectrometry; Exotot, total TG weight loss for the temperature interval 200–650 °C; CP-MAS, cross polarization-magic angle spinning.

0165-2370/$ – see front matter © 2008 Elsevier B.V. All rights reserved.
doi:10.1016/j.jaap.2008.11.019

environmental samples may differ from method to method depending upon the sample treatment used [2]. In addition, BC is studied in a variety of isolated scientific fields, with the result that no generally accepted analytical protocols have been developed. BC quantification in complex matrices is impeded by methodological problems related to the analytical windows of the different methods, which only allow for the quantification of one part of the BC continuum [2]. A further difficulty lies in the occurrence of refractory organic materials that analytically behave like BC but do not derive from combustion and thus may lead to an overestimation of BC content. Among such materials are for example coals, kerogens or even melanoidins, although the latter may partly derive from the thermally induced Maillard reaction between carbohydrates and amino compounds during burning [3].

Therefore, there is a need to develop accurate and comparable analytical protocols to determine the amount of BC stored in different environmental matrices ([4] and references therein). Additionally, the impact of interfering non-combustion-derived refractory organic matter on the quantification has to be elucidated. However, despite significant improvements achieved in the analytical techniques and considerable efforts to characterise sedimentary organic carbon, a large fraction of it remains biochemically uncharacterised [5] and there is not a single accepted method able to detect and quantify BC [6,7].

The steering committee of the "BC-Ring Trial" (BC Ring-Trial. www.geo.unizh.ch/phys/bc/ringtrial.html) recommended the needed of studying a set of four materials that are expected to interfere with the BC determination. Those materials have high ROM content and properties similar to those of BC-rich materials [8]. Although they should not contain BC, due to the ambiguities in the BC definition and the differences between the methodologies used, those potentially interfering materials share some properties with BC materials (high C content, low lightness values and high aromaticity) that are used for certain BC quantification methods [9].

The interfering materials studied in this work were those recommended by the "BC-Ring Trial" and consist of an artificially produced melanoidin (mel), a sample of shale very rich in kerogen type I from Utah (USA), a lignite coal from North Dakota (USA) and a bituminous coal sampled in Virginia (USA).

The main objectives of this study were (a) to obtain additional information about the chemical composition of those materials by the combined use of elemental analysis, thermogravimetry–differential scanning calorimetry (TG–DSC) and pyrolysis coupled with gas chromatography–mass spectrometry (Py-GC/MS) and (b) to determine if the latter can be used to detect BC in complex materials. Additionally, solid-state ^{13}C nuclear magnetic resonance (NMR) spectroscopy was applied to allow the complementary comparison of those data with the overall bulk chemical composition of the samples.

Thermal analysis methods, specifically thermogravimetry–differential scanning calorimetry, have been used to characterise chemical changes in the organic matter fractions of soils and sediments, degraded plant tissue or compost [10–12]. TG–DSC has also been used to compare the proportions of reactive and more stable components in organic matter fractions under contrasting conditions [12,13], and recently to different forms of black carbon [14]. Analytical pyrolysis coupled with gas chromatography–mass spectrometry, has been successfully applied in previous studies for the identification of typical constituents in the refractory fraction of soils [15] and sediments containing BC [16]. Py-GC/MS has also been used to characterise resilient OM [17–19], cuticular resilient plant materials [20], and as a complementary tool to analyze biomarkers in kerogens [21] and fossil remains [22].

2. Materials and methods

2.1. Materials

The samples presented in this study were supplied by the Geography Department, University of Zurich, Switzerland (Dr. M. Schmidt). They are described as follow:

(i) Melanoidin sample was artificially produced in the Geography Department of the University of Zurich by following a simple method based on the reaction between urea and glucose in distilled water during 30 days at 90 °C [23]. Originally used to represent a group of organic materials which may interfere in the separation of BC from the rest of non-BC ROM. Melanoidins are complex, insoluble macromolecules, highly resistant to chemical degradation, formed by random condensation of monomers and other alteration products of amino acids and carbohydrates [24]. They were artificially produced by Maillard in 1917 [24], but since that other synthesis procedures have been published [25,26]. However, during heating of organic matter such products can be formed naturally [3].

(ii) The kerogen sample was obtained from the Mahogany zone of the Green River Shale formation (Utah, USA) and has been characterised formerly by Bishop et al. [27]. This geologic material is a kerogen type I, immature, highly bituminous and has been used as a reference material by the US Geological Survey (code SGR-1) Box 25046, Denver, USA (http://minerals.cr.usgs.gov).

(iii) The lignite sample was selected because it represents the end part of the wide range of carbons is a soft, brownish-black coal in which the alteration of vegetable matter has proceeded further than in peat but not as far as in bituminous coal, it is also called *brown coal*. This lignite was sampled in the Mercer County (North Dakota, USA) and provided by *The Argonne National Laboratory* (USA) (http://www.anl.gov/).

(iv) The bituminous coal sample consists of soft coal material from the Buchanan County (Virginia, USA), that developed from deeply buried lignite through heat and pressure; it was supplied by *The Argonne National Laboratory* (USA). A more detailed description of those materials can be found in Refs. [4,28].

2.2. Analysis

2.2.1. Elemental analysis

Carbon and nitrogen analysis was performed on a Carlo-Erba NA 1500 Series 2 Elemental Analyzer (CE Elantech, Inc., Lakewood, NJ). Samples were analyzed in duplicate.

2.2.2. Thermogravimetry–differential scanning calorimetry (TG–DSC)

Thermal analysis was carried out by a Netzsch STA 449C Jupiter TG–DSC system [16]. Approximately 10 mg of soil sample were weighed into an alumina crucible and analyzed in duplicate (each analysis takes 2–3 h). Samples were heated at 20 °C min^{-1}, from ambient temperature to 990 °C under flowing 20% oxygen in helium (50 cm^3 min^{-1}). The TG and DSC signals were exported to the NETZSCH software for analysis versus temperature. In accordance with previous descriptions [11,12], thermal analysis allows distinction of labile soil OM (decomposes between 200 and 380 °C), recalcitrant OM (weight losses observed between 380 and 475 °C), and refractory OM (decomposes between 475 and 650 °C). The weight losses observed within these temperature ranges are referred to respectively as Exo 1, Exo 2 and Exo 3, as relative proportions of the total weight loss (Exotot) between 200 and 650 °C [11,13,14].

2.2.3. Pyrolysis-gas chromatography–mass spectrometry

To achieve a more detailed molecular characterisation of the samples, bulk samples were analyzed by using a pyrolyzer (model 2020, Frontier Laboratories Ltd. Fukushima, Japan). The gases evolved during pyrolysis were separated using a fused silica HP 5MS capillary column (30 m × 250 μm × 0.25 μm inner diameter). The detector consisted of an Agilent 5973 mass selective detector (Electron Impact at 70 eV) (Agilent, Santa Clara, CA). Depending on the C content, for all experiments between 0.4 and 2 mg of a sample material were placed in small platinum capsules. The flash Pyrolysis shot was carried out at 500 °C. The GC–MS conditions were the same for all the samples, keeping the oven temperature at 40 °C for 1 min and then increasing it up to 100 °C at steps of 30 °C min^{-1}, from 100 to 500 °C with 20 °C min^{-1}, keeping it isothermal at 500 °C for 2 min. The carrier gas used was helium with a controlled flow rate of 1 ml min^{-1}.

The identification of individual compounds was achieved by single ion monitoring for different homologous series, low-resolution mass spectrometry and comparison with published and stored (NIST and Wiley libraries) data. The sum of all identified pyrolysis products was defined as 100%, from which the relative amount of each pyrolysis product was calculated, and the data for two repetitive pyrolysis experiments were averaged. Note that this represents the quantification of fragment abundance, and not of weight percentage, peaks corresponding to column fragments and CO_2 have been removed from the list of identified compounds (Table 3). Quantified pyrolysis fragments ranged in molecular weight from about 45 to700 Da. Thus, the abundance of a fragment is not directly proportional to the carbon content of this fragment. However conversion of pyrolysis fragment abundance to functional group abundance has been discussed by Nelson and Baldock [29] to enable a comparison of pyrolysis data with other spectroscopic methods, such as ^{13}C NMR.

2.2.4. ^{13}C NMR spectroscopy

The solid-state cross polarization-magic angle spinning (CP-MAS) ^{13}C NMR spectra were obtained on a Bruker DSX 200 NMR spectrometer. Samples were freeze-dried before NMR measurement. Approximately 300 mg of dry sample was packed into a 7 mm zirconium rotor with a Kel-F cap. The CP-MAS was carried out with a spinning speed of 6.8 kHz, a contact time of 1 s and a pulse delay of 1 s. The ^{13}C chemical shifts were referenced to tetramethylsilane (=0 ppm) and adjusted with glycine (=176.04 ppm) as an external standard. The acquisition parameters were as follows: spectral frequency of 50.3 MHz for ^{13}C and 200 MHz for ^{1}H. For quantification of the relative proportion of the organic C groups, the solid-state ^{13}C NMR spectra were divided into chemical shift regions which were integrated using a modified integration routine supplied with the instrument software [30]. The regions from 245 to 185 ppm and from 185 to 160 ppm are assigned to carbonyl and carboxyl/amide C. Between 160 and 110 ppm resonance lines of olefins and aromatic C are detected. In spectra of unburned soil organic matter or plant residues and fire-unaffected soils, O-alkyl and N-alkyl-C signals determines the intensity between 110 and 60 ppm and from 60 to 45 ppm. Resonances of alkyl C are expected between 45 and 0 ppm. Owing to insufficient averaging of the chemical shift anisotropy at a spinning speed of 6.8 kHz, spinning side bands (ssb) of the aromatic C signals occurred at a frequency distance of the spinning speed at both sides of the central signal (300 to 245 ppm and 0 to −50 ppm). The ssbs of the carboxyl C signal attribute to the intensity in the chemical shift region between 325 and 300 ppm and between 45 and 0 ppm according to Ref. [31]. Their contributions were considered by adding their intensities to that of the parent signal. The intensity of the ssbs of alkyl and O-alkyl C could not be distinguished from the noise and thus were not considered for the determination of the ^{13}C NMR intensity distribution.

3. Results

3.1. Elemental analysis

Table 1 shows the results obtained from elemental (C, N) analysis of samples. C values ranged 846.7–272.3 g kg^{-1} for the bituminous coal and shale samples respectively, confirming the richness in C of all the samples. The C contents of the bituminous coal, the lignite and the shale decrease in accordance with their coal rank.

As it was expected the melanoidin sample contained a higher N content (86.5 g kg^{-1}). On the other hand, C/N ratios show the wide variability in the spectrum of materials potentially interfering with BC.

3.2. Thermal analysis (TG–DSC)

Table 2 lists the results corresponding to TG–DSC analysis of samples. Fig. 1 shows DSC curves indicating that the oxidation begins at temperatures as low as 200 °C, and with weight losses complete by 550 °C. The melanoidin and shale samples show exothermic reactions at temperatures associated with labile materials (200–375 °C) and recalcitrant materials, whereas the bituminous coal shows a maximum reaction temperature at 560 °C. Most of these samples exhibit weight losses and exothermic reactions in all three C pools, but of varying proportions (as see in Table 2). Summarising the DSC data indicates a higher content of labile OM in the melanoidin and the shale samples, than in the lignite and the bituminous coal, in which ROM is the predominant form of OM. However, an exothermic peak at temperatures higher than 550 °C reveals a high thermal recalcitrance of the latter, questioning if this sole criteria is appropriate to distinguish BC materials produced by burning and combustion. In fact the thermograms of the bituminous coal are similar to those obtained for some BC-rich sample described in the literature [14].

3.3. Analytical pyrolysis

Due to the complexity of the total ion current (TIC) traces and the number of identified compounds, the pyrograms are separated

Table 1
Carbon, nitrogen and C/N ratio values of bulk samples.

Sample	C (g kg^{-1})	N (g kg^{-1})	C/N
Melanoidin	542.6	86.5	6.3
Shale	272.3	8.4	32.4
Lignite	583.6	10.0	58.4
Bituminous coal	846.7	8.2	103.3

Table 2
Comparative thermogravimetry (TG) weight loss (%) for the temperature interval 50–800 °C (total TG loss), direct and relative weight losses (%) of temperature intervals Exo 1 (200–380 °C), Exo 2 (380–475 °C) and Exo 3 (475–650 °C).

Range T (°C)	Melanoidin	Shale	Lignite	Bituminous coal
Total TG loss	91.5	35.6	92.1	83.2
200–380	31.1	14.8	23.7	1.5
380–475	19.7	15.4	37.5	8.5
475–650	24.6	3.0	19.1	73.0
Exo 1	41.2	44.6	29.5	1.8
Exo 2	26.1	46.4	46.7	10.2
Exo 3	32.6	9.0	23.8	88.0

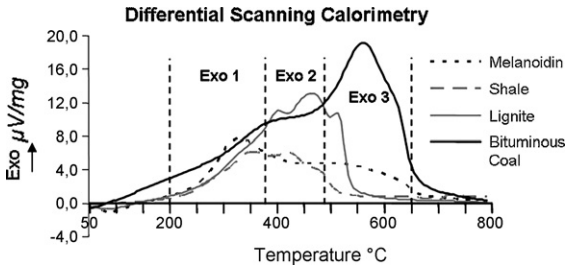

Fig. 1. Differential scanning calorimetric (DSC) curves of samples within the range from 50 to 800 °C.

in two figures (Fig. 2a and b). Fig. 2a shows the TIC pyrogram of the shale and the melanoidin samples, whereas the lignite and the bituminous coal samples are depicted in Fig. 2b. Note that the pyrogram of the melanoidin sample is only given until minute 12 because no more compounds were identified afterwards. The 156 identified compounds are listed in Table 3, depending upon their structure and possible precursors, the pyrolysis products are grouped into five compound classes in: alkanes (●) and alkenes (○) (58 different compounds identified), carbohydrates (C1–C14), proteins (P1–P26), aromatics without a specific origin (A1–A51) and others (peaks 1–7), the last group includes a variety of compounds including some lipids (peaks 3, 5–7 in Table 3).

The possible origin of the products has been attributed following known relationships between pyrolysis products and biological precursors composing OM [19–22,13].

The pyrolysates generated from the four samples are quite different. The trace for melanoidin (Fig. 2a) reveals an important contribution of carbohydrates structures (see peaks C1–C10 in Fig. 2a), which accounts for more than 60% (Table 4), furanic products in such pyrolysates are derived from sugar moieties [32]. Nitrogen bearing structures (P1–P26 in Table 3) comprise more than 18% (Table 4), whereas signals for alkanes or alkenes were missing. Thus Table 3 and Fig. 2a show that most of those compounds, for example furanes (see C1–C5 compounds), pyrrols and pyridines (see Table 3), are detected only in this sample. This could be indicative of the different nature and origin of the OM present in this sample.

The program of the shale sample (Fig. 2a) is dominated by alkane–alkene doublets (over 30% in Table 4) and aromatic structures (over 60%). The latter include benzenes, indenes and naphthalene as the most abundant, but also hopanes and cholestane (peaks 5–7) were detected, which are compounds typically found in the pyrolysis of shale samples. In addition to normal hydrocarbons, phytane was also identified (Fig. 2a) which is commonly observed as pyrolysis product of macromolecular natural OM and originate from the cracking of the isoprenic phytyl chain of chlorophyll [33]. Pristane/phytane ratios have been used as a measure of the sediment oxicity [34,35]. In this case the unique

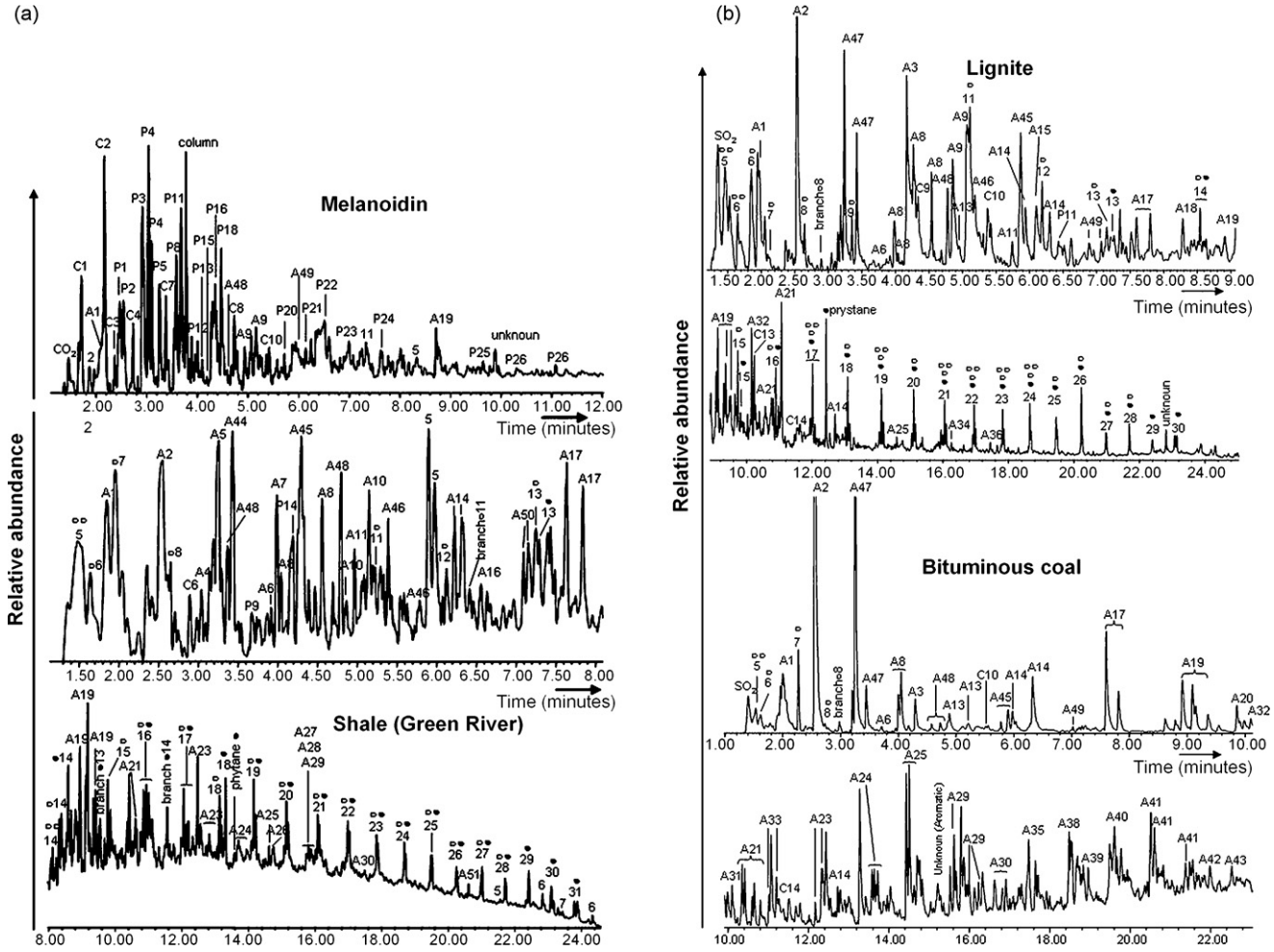

Fig. 2. (a) Total ion chromatograms pyrolysis-gas chromatography/mass spectroscopy from lignite and bituminous coal samples. The numbers over the peaks refer to compounds listed in Table 3. (b) Total ion chromatograms pyrolysis-gas chromatography/mass spectroscopy from melanoidin and shale samples. The numbers over the peaks refer to compounds listed in Table 3.

Table 3
Peak identification and relative content (%) of pyrolysis gas chromatography–mass spectrometry products by component classes.

Peak label	Compound	Sample			
		Shale	Melanoidin	Lignite	Bituminous coal
Protein-derived structures					
P1	3-Methyl-1H-pyrrole		1.57		
P2	Pyridine		3.50		
P3	4-Methylpyridine		7.30		
P4	1-Methyl-1H-pirrole		11.49		
P5	2-Methylpyridine		3.95		
P6	2,6-Dimethylpyridine		2.18		
P7	2-Ethylpyridine		1.78		
P8	2,6-Dimethylpyrazine		4.90		
P9	2,3-Dimethyl-1H-pirrole	0.56			
P10	Ethenylpyrazine		0.80		
P11	3,5-Dimethyl-1H-pirrole	0.31	6.15		
P12	3-Ethyl-1H-pirrole		0.51		
P13	2-Ethyl, 6-methylpyridine		0.67		
P14	*x*,*x*,*x*-Trimethylpyridine	1.12	1.25		
P15	2-Ethyl-6-methylpyrazine		1.53		
P16	2,3,5-Trimethylpyrazine		1.73		
P17	4-Ethyl-2-methylpirrole		0.83		
P18	2,3,4-Trimethylpirrole		3.34		
P19	2-Ethenyl-5-methylpyrazine		0.33		
P20	Indole		0.61		
P21	4-Methoxybenzenamine		0.75		
P22	2-H-1-Benzopyran-2-ona		1.76		
P23	3-Methyl-indole		1.23		
P24	Dimethyl-indole		0.76		
P25	*x*,*x*-Dimethylindole		2.52		
P26	1,2,3-Trimethyl-1H-indole		0.60		
	Total	1.99	62.03	–	–
Carbohydrates-derived structures					
C1	2-Methylfurane		4.65		
C2	2,5-Dimethylfurane		8.28		
C3	Vinylfurane		0.48		
C4	2-Ethyl-5-methylfurane		1.31		
C5	2,3,5-Trimethylfurane		0.50		
C6	3,5-Dimethylcyclohexene	0.78			
C7	2-Methyl-5-propylfurane		0.41		
C8	2,3-Dimethyl-2-cyclopenten-1-one		1.99		
C9	Benzofurane			1.64	
C10	*x*-Methylbenzofurane		1.10	2.61	
C11	*x*,*x*-Dimethylbenzofurane			0.71	
C12	*x*,*x*-Dimethyltiophene			0.08	
C13	Dibenzofurane			0.23	
C14	4-Methyl-dibenzofurane			0.25	0.26
	Total	0.78	18.72	5.52	0.26
Alkanes and alkenes					
○○5	1,3-Pentadiene	4.77		3.34	1.56
○6	1-Hexene	2.15		1.11	0.15
○○6	1,3-Hexadiene			3.46	0.34
○7	1-Heptene	1.27		0.74	2.05
○8	1-Octene	0.89		0.65	0.24
branch○8	2-Methyl-1-octene			0.30	0.26
○9	1-Nonene	1.17		0.63	
○10	1-Decene	0.88			
●10	Decane	0.52		0.52	
○11	1-Undecene	0.44		3.56	
○12	1-Dodecene	1.49		1.20	
branch○11	Methyl-undecene	0.16			
○13	1-Tridecene	1.21		0.86	
●13	Tridecane	0.49		0.18	
○○14	Tetradecadiene	0.32		0.22	
○14	1-Tetradecene	1.02		0.63	
●14	Tetradecane	0.99		0.18	
branch●12	4,6-Dimethyldodecane	0.60			
○○15	1,13-Pentadecadiene	0.35			
○15	1-Pentadecene	0.81			
●15	Pentadecane	0.38		0.16	
○○16	*x*,*x*-Hexadecadiene	0.78			
○16	1-Hexadecene	0.90		0.62	
●16	Hexadecane	0.67		0.23	
branch●16	3-Methylhexadecane	0.56			

Table 3 (*Continued*)

Peak label	Compound	Sample			
		Shale	Melanoidin	Lignite	Bituminous coal
○17	1-Heptadecene	0.82		0.77	
●17	Heptadecane	0.41		0.17	
●pristane	Pristane			1.06	
○18	1-Octadecene	0.65		0.60	
●18	Octadecane	0.26		0.15	
●phytane	Phytane	0.83			
○○19	Nonadecadiene	0.21		0.14	
○19	1-Nonadecene	0.93		0.49	
●19	Nonadecane	0.45		0.21	
○20	1-Eicosene	0.74		0.74	
●20	Eicosane	0.46		0.21	
○○21	Heneicosadiene	0.12		0.09	
○21	1-Heneicosene	0.47		0.37	
●21	Heneicosane	0.36		0.19	
○○22	1,21-Docosadiene			0.15	
○22	1-Docosene	0.59		0.45	
●22	Docosane	0.45		0.19	
○23	1-Tricosene	0.31		0.32	
●23	Tricosane	0.32		0.20	
○24	1-Tetracosene	0.38		0.41	
●24	Tetracosane	0.27		0.17	
○25	1-Pentacosene	0.35		0.38	
●25	Pentacosane	0.35		0.26	
○26	1-Hexacosene	0.25		0.68	
●26	Hexacosane	0.17		0.22	
○27	1-Heptacosane	0.16		0.27	
●27	Heptacosane	0.26		0.21	
○28	1-Octacosene	0.19		0.29	
●28	Octacosane	0.17		0.13	
●29	Nonacosane	0.45		0.28	
●30	Triacontane	0.35		0.27	
●31	Henetriacontane	0.16			
●32	Dotriacontane	0.06			
58 compounds	Total alkanes	8.83	–	5.19	–
	Total alkenes	25.93	–	23.44	4.61
	Total	34.76	–	28.63	4.61
Aromatic structures					
A1	Benzene	5.15	0.80	4.01	4.37
A2	Toluene	5.31	3.89	7.42	17.54
A3	Phenol		1.67	5.79	
A4	Ethylbenzene	1.35			
A5	1,3-Dimethylbenzene	3.35			
A6	2-Propyl-benzene	0.44		0.12	0.07
A7	1-Ethyl, 2-methylbenzene	2.05			
A8	*x,x,x*-Trimethylbenzene	3.60		5.82	4.33
A9	*x*-Cresol		5.03	7.78	0.32
A10	*x*-Isopropyl-benzene	0.97			
A11	*x,x,x,x*-Tetramethylbenzene	0.40		0.12	
A12	*p*-Ethoxytoluene		0.99		
A13	*x*-Buthylbenzene			0.20	1.23
A14	Naphthalene	1.73		1.52	3.81
A15	*x*-Ethylphenol			2.14	
A16	*x,x,x*-Trimethylphenol	1.00			
A17	*x*-Methylnaphthalene	4.83		1.84	6.10
A18	*x,x*-Dihydro-*x,x*-dimethylnaphthalene			1.00	
A19	*x,x*-Dimethylnaphthalene	6.56	0.59	3.52	6.52
A20	1,1′-Biphenyle	0.42			0.95
A21	*x,x,x*-Trimethylnaphthalene	1.83		2.12	2.14
A22	9-H-Fluorene	0.35			
A23	*x*-Methyl-9-H-fluorene	1.16		0.21	2.19
A24	2,3-Dimethyl-9-H-fluorene	0.20		0.14	2.54
A25	*x*-Methylanthracene	0.30		0.13	4.47
A26	*x*-Methylphenanthrene	0.79			
A27	2-Ethylanthracene	0.17			
A28	Isocopaline	0.19			
A29	*x,x*-Dimethylphenanthrene	0.58			4.00
A30	Benzofluorene	0.17			2.00
A31	*x*-Isopropylnaphthalene				0.71
A32	*x*-Methyl-1,1′-biphenyl			1.02	0.37
A33	*x,x*-Dimethyl-*x,x*-biphenyl				1.90
A34	Pyrene			0.11	
A35	*x,x,x*-Trimethylphenanthrene				0.89
A36	*x,x,x,x*-Tetramethylphenanthrene			0.16	0.30
A37	1-Methylpyrene				0.38

Table 3 (*Continued*)

Peak label	Compound	Sample			
		Shale	Melanoidin	Lignite	Bituminous coal
A38	*x*,*x*-Dimethylpyrene				2.99
A39	Benzo(b)naphto (2,3-d)tiophene				0.48
A40	*x*-Methyl-chrysene				2.35
A41	Dimethylbenzo(c)phenanthrene				2.08
A42	Benzo(K)fluorantene				0.46
A43	Benzo(a)pyrene				0.39
A44	Styrene	3.30			
A45	*p*-Methyl styrene	1.44			
A46	*x*,*x*-Dimethylstyrene	0.75		1.09	
A47	*x*,*x*-Xylene			7.34	12.29
A48	Indene	2.45	1.03	1.74	0.63
A49	*x*-Methyl-1H-indene	6.41	1.18	5.17	1.66
A50	*x*,*x*-Dimethyl-1H-indene	2.92		0.20	
A51	1,2,3-Trimethylindene	0.37			
	Total	60.54	15.18	60.71	90.45
Other structures – different origin					
1	SO_2			3.26	2.26
2	1-Methyl,1,3-cyclopentadiene		1.63		
3	Acetic acid		0.89		
4	8-Methylquinoline		0.90		
5	α-Cholestane	0.07			
6	Hopane	0.65			
7	*x*-α-Stigmastane	0.32			
	Total	1.04	3.42	3.26	2.26

Results are given in %, related to the total area of released compounds by Py-GC/MS shown in Fig. 2a and b.

presence of phytane could suggest that the diagenesis occurred in predominantly anoxic depositional environments.

The pyrolysates of the lignite and the bituminous coal (Fig. 2b) reveal a high proportion of aromatic structures representing >90% in the bituminous coal and >69% in the lignite. In both cases the aromatic compounds mainly derived from benzene (particularly xylenes), alkyl-benzenes, toluene and phenol whereas PAHs, resulting most of the peaks from A14 to A43 in Table 3, are more abundant in the bituminous coal. This may indicate a greater condensation degree of the latter. A direct relationship between the percentages of aromatic structures measured by Py-GC/MS, and the C/N ratios (Table 1) was obtained. Especially for the lignite, the relative high abundance of aliphatic material, including chlorophyll-derived pristane, is remarkable (alkanes + alkenes > 28%). No protein-derived structures were identified.

3.4. ^{13}C NMR spectroscopy

Fig. 3 shows the solid-state ^{13}C NMR spectra of the samples. Their relative intensity distribution is given in Table 5. In contrast to the spectra presented by Hammes et al. [9], obtained with a spinning speed of 5 kHz, those of the present study were acquired with 6.8 kHz to further minimize quantification problems related to spinning side bands. With the exception of the Green River Shale, all spectra show high intensity in the chemical shift region corresponding to aromatic C. The spectrum of the Green River Shale is dominated by a signal at 28 ppm in the region of alkyl C, confirming the pyrolysis data and supporting the paraffinic character of those fossilized algal residues [36]. The spectrum of the melanoidin reveals remains of O-alkyl C (110 to 45 ppm). Together with the signal at 200 and 154 ppm assignable to aldehyde/keto C and O-aryl C and this finding is in agreement with the furane/pyrane moieties detected as pyrolysis products of carbohydrates. However, signals of N-heterocyclic C will be embraced by the broad aromatic C signals. The intensity in the region between 45 and 0 ppm is split into two signals, one at 31 ppm and the other around 22 ppm. The latter is indicative for acetyl C. Compared to previously published spectra for this sample [9], ours reveals a higher relative intensity in the region of alkyl C and lower in that of O-alkyl C. This is possibly due to the higher spinning speed used in our experiments (6.8 kHz), being able to avoid spinning side bands of the alkyl-C region and the whole intensity occurs in the region of the parent signal. Comparable to the pyrogram of the lignite, its NMR spectrum reveals signals typical for lignin remains at 142 ppm (O-aryl C), 54 ppm (methoxyl C) and 29 ppm (alkyl side chain). The signals at 180 and 203 ppm assignable to carbonyl C indicate that some of those remains are oxidized.

Table 4
Summarised results of pyrolysis–GC/MS by component classes (in capitals).[a]

	Sample			
	Shale	Melanoidin	Lignite	Bituminous coal
ALKANES and ALKENES	34.76	–	28.63	4.61
PROTEIN STRUCTURES	1.99	62.03	–	–
AROMATIC STRUCTURES	60.54	15.18	60.71	90.45
CARBOHYDRATES	0.78	18.72	5.52	0.26
OTHERS	1.04	3.42	3.26	2.26

[a] Results are given in % relative to total peak area of identified compounds.

4. Discussion

In spite of the fact that analytical pyrolysis detects only the part of the whole OM, that can be volatilized, and of the well-known problem of decarboxylation of compounds at elevated temperatures [37], the Py-GC/MS results match reasonably well with the relative contributions of the different C groups to the total C as determined by solid-state ^{13}C NMR spectroscopy (Table 5). Both techniques confirm the high aromaticity of the bituminous coal and the lignite, which contributes to the high thermal stability demonstrated by the TG–DSC analysis. Note that the latter is in the range recently determined for BC-rich samples [13]. Py-GC/MS of the coal samples further reveals that a considerable part of the

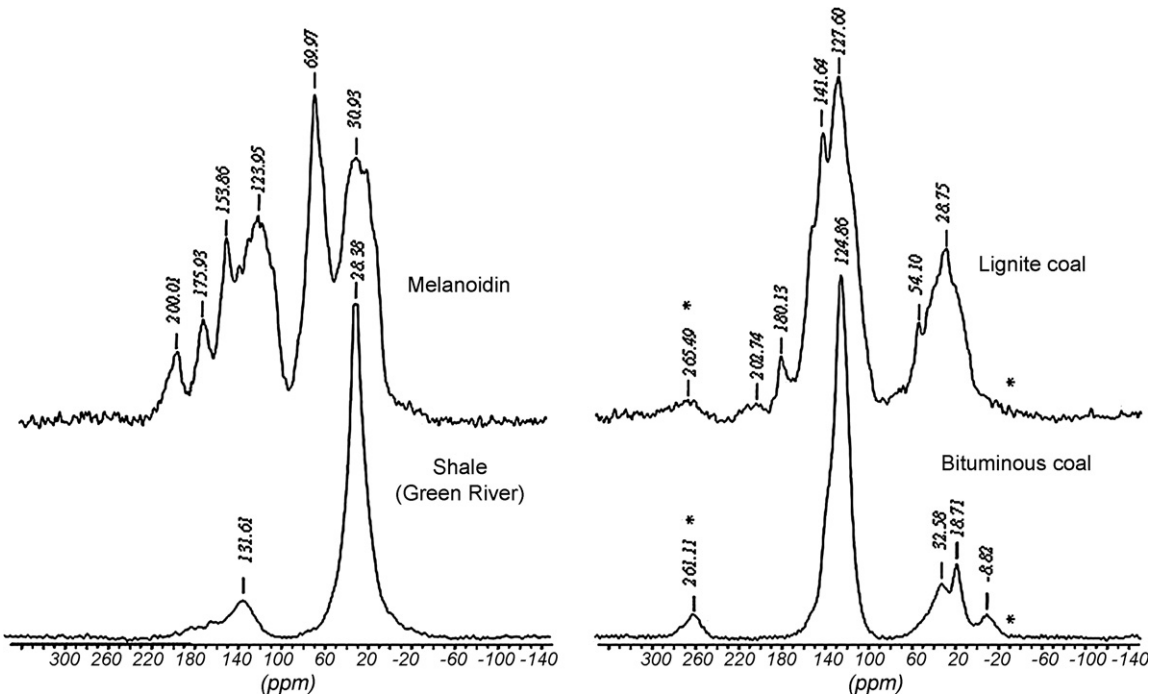

Fig. 3. Solid-state ^{13}C NMR spectra of samples.

aromatic compounds are lignin-derived products. Most of these products were also observed among the pyrolysis products of the BC-rich samples [13]. The occurrence of those compounds in both materials can be explained by the high resistance of lignin against combustion [38] but also against diagenetic/catagenetic alterations [39]. Accordingly, our data are in line with the suggestion that lignin degradation products are not only mayor constituents of low and medium rank coals [39] but also represent an important integral part of BC material [40]. This however, aggravates the discrimination between the two sources of aromatic rich refractory material solely by means of chemical characterisation.

Both, analytical pyrolysis and ^{13}C NMR spectroscopy confirm a high contribution of long alkyl-C chains in the shale sample. Due to their high hydrophobicity they survive chemical oxidation treatments after which the C content of the residue is often used as means for BC quantification [4]. However, in recent aquatic sediments [41] and in some soils, the presence of such paraffinic structures [42] is a common feature. In BC quantification approaches that use thermal oxidation those compounds will contribute to the ROM fraction. They cause an overestimation of the actual BC determined by chemical oxidation methods [4].

With respect to the melanoidin sample, TG–DSC confirmed its relative low thermal stability. Additionally the pyrolysis product and the NMR spectroscopy demonstrate a considerable proportion of so-called Maillard products consisting of pyranes, furans and N-heterocyclic residues. Such structures are commonly not considered to be part of BC [3]. However, charring plant residues or humic substances results in pyrogenic organic matter with low carbon to nitrogen that contain such Maillard products [31,43,44]. This demonstrates that in spite of their low TG-stability, those products cannot be neglected if one seeks a better understanding of the structural properties of BC [45].

Table 5
Solid-state CP-MAS ^{13}C NMR intensity distribution of studied samples.

	Sample				
	Carbonyl C	Aryl C	O-alkyl C	N-alkyl and methoxyl C	Alkyl C
	ppm range				
	210–160	160–110	110–60	60–45	45–0
Melanoidin	11.3	29.8	23.0	7.5	28.3
Shale	1.8	14.9	4.2	6.8	72.4
Lignite	7.9	56.5	9.1	5.2	21.3
Bituminous coal	0.6	77.1	3.1	2.0	17.2

5. Conclusions

The present study demonstrates that analytical pyrolysis together with ^{13}C NMR spectroscopy and TG–DSC are complementary techniques for the study of the chemical composition and thermal stability of ROM. Applying those techniques to four samples of non-combustion-derived refractory organic material revealed that a considerable fraction of their constituents is also present in the so-called BC samples. They even may be part of BC structure, as has been recently suggested by Knicker [45]. The chemical similarity of the refractory constituents of both, combustion- and non-combustion-derived materials, may be the main reason for the difficulties in identifying and quantifying BC by conventional methods that assumes that BC is mainly composed of highly condensed polyaromatic units. The latter, on the other hand could not be confirmed by our study. The obtained results indicates that current BC-identification approaches have to be revisited and modified to account for a more heterogeneous less condensed BC nature.

Acknowledgements

We thank Dr. C. Rumpel and Dr. M.F. Dignac from INRA (France) for supporting us in the elemental analysis. The Spanish Ministry of Education provided a fellowship to J.M. de la Rosa for this research (BES-2003-1900). We acknowledge support from the Royal Society (Joint Project 2005/R3-JP) and CSIC (Proyectos Conjuntos 2005GB0098).

References

[1] E.D. Goldberg, Black Carbon in the Environment: Properties and Distribution, John Wiley & Sons, New York, 1985.
[2] C.A. Masiello, Mar. Chem. 92 (2004) 201.
[3] R. Ikan, The Maillard Reaction; Consequences for the Chemical and Life Science, John Wiley & Sons, Chichester, 1996;
M.W.I. Schmidt, A.G. Noack, Global Biochem. Cycles 14 (2000) 777.
[4] K. Hammes, M.W.I. Schmidt, R.J. Smernik, L.A.R. Currie, W.P. Ball, T.H. Nguyen, P. Louchouarn, S. Houel, Ö. Gustafsson, M. Elmquist, G. Cornelissen, J.O. Skjemstad, C.A. Masiello, J. Song, P. Peng, S. Mitra, J.C. Dunn, P.G. Hatcher, W.C. Hockaday, D.M. Smith, C. Hartkopf-Fröder, A. Böhmer, B. Lüer, B.J. Huebert, W. Amelung, S. Brodowski, L. Huang, W. Zhang, P.M. Gschwend, D.X. Flores-Cervantes, C. Largeau, J.N. Rouzaud, C. Rumpel, G. Guggenberger, K. Kaiser, A. Rodionov, F.J. Gonzalez-Vila, J.A. Gonzalez-Perez, J.M. De la Rosa, D.A.C. Manning, E. López-Capél, L. Ding, Global Biochem. Cycles 21 (2007), doi:10.1029/2006GB002914.
[5] J.I. Hedges, R.G. Keil, R. Benner, Org. Geochem. 27 (1997) 195.
[6] M.W.I. Schmidt, J.O. Skjemstad, C.I. Czimczik, B. Glaser, K.M. Prentice, Y. Gelinas, T.A.J. Kuhlbusch, Global Biogeochem. Cycles 15 (2001) 163.
[7] C.A. Masiello, E.R.M. Druffel, Science 280 (1998) 1911.
[8] K. Hammes, R.J. Smernik, J.O. Skjemstad, A. Herzog, U.F. Vogt, M.W.I. Schmidt, Org. Geochem. 37 (2006) 1629.
[9] K. Hammes, R.J. Smernik, J.O. Skjemstad, M.W.I. Schmidt, Appl. Geochem. 23 (2008) 2113.
[10] M.T. Dell'Abate, S. Canali, A. Trinchera, A. Benedetti, P. Sequi, J. Ther. Anal. Cal. 61 (2000) 389.
[11] E. Lopez-Capel, S.P. Sohi, J.L. Gaunt, D.A.C. Manning, Soil Sci. Soc. Am. J. 69 (2005) 136.
[12] E. Lopez-Capel, G.D. Abbott, K.M. Thomas, D.A.C. Manning, J. Anal. Appl. Pyrol. 75 (2006) 82.
[13] J.M. De la Rosa, H. Knicker, E. López-Capel, D.A.C. Manning, J.A. González-Pérez, F.J. González-Vila, Soil Sci. Soc. Am. J. 72 (2008) 258.
[14] J. Leifeld, Org. Geochem. 38 (2007) 112.
[15] F.J. González-Vila, P. Tinoco, G. Almendros, F. Martin, J. Agric. Food Chem. 49 (2001) 1128.
[16] J.C. Del Rio, D.E. McKinney, H. Knicker, M.A. Nanny, R.D. Minard, P.G. Hatcher, J. Chromatogr. A 823 (1998) 433.
[17] F.J. González-Vila, A. Amblès, J.C. del Río, L. Grasset, J. Anal. Appl. Pyrol. 58–59 (2001) 315.
[18] G. Almendros, J. Dorado, F.J. González-Vila, F. Martín, J. Sanz, C. Álvarez-Ramis, L. Stuchlik, Fuel 78 (1999) 745.
[19] C. Saiz-Jimenez, J.W. de Leeuw, Org. Geochem. 6 (1984) 287.
[20] C. Saiz-Jimenez, J.W. de Leeuw, J. Anal. Appl. Pyrol. 9 (1986) 99.
[21] Y. Coban-Yildiz, D. Fabbri, D. Tartari, S. Tugrul, A.F. Gaines, Org. Geochem. 31 (2000) 1627.
[22] M.J. Simpson, B. Chefetz, A.P. Deshmukh, P.G. Hatcher, Mar. Environ. Res. 59 (2005) 139.
[23] M. Elmquist, Ö. Gustafsson, P. Andersson, Limnol. Oceanogr. 2 (2004) 417.
[24] L.C. Maillard, Ann. Chim. (Paris) 7 (1917) 113.
[25] B. Allard, J. Templier, C. Largeau, Org. Geochem. 26 (1997) 691.
[26] K. Olsson, P.A. Pernemalm, O. Theander, Acta Chem. Scand. 32 (1978) 249.
[27] A.N. Bishop, G.D. Love, A.D. McAulay, C.E. Snape, P. Farrimond, Org. Geochem. 29 (1998) 989.
[28] A.C. Scott, I.J. Glasspool, Int. J. Coal Geol. 70 (2007) 55.
[29] P.N. Nelson, J.A. Baldock, Biogeochemistry 72 (2005) 1.
[30] M.A. Wilson, Techniques and Applications in Geochemistry and Soil Chemistry, Pergamon Press, New York, 1987.
[31] H. Knicker, K.-U. Totsche, G. Almendros, F.J. González-Vila, Org. Geochem. 36 (2005) 1359.
[32] I. Pastorova, R.E. Botto, P.E. Arisz, J.J. Boon, Carbohydr. Res. 262 (1994) 27.
[33] M. Ishiwatari, R. Ishiwatari, H. Sakashita, T. Tatsumi, H. Tominaga, J. Anal. Appl. Pyrol. 18 (1991) 207.
[34] B.M. Didyk, B.R.T. Simoneit, S.C. Brassell, Nature 272 (1978) 216.
[35] R.B. Gagosian, S.O. Smith, C. Lee, J.W. Farrington, N.M. Frew, Adv. Org. Geochem. 12 (1980) 407.
[36] L.L. Ingram, J. Ellis, P.T. Crisp, A. Cook, Chem. Geol. 38 (1983) 185.
[37] F. Martín, F.J. González-Vila, J.C. del Río, T. Verdejo, J. Anal. Appl. Pyrol. 28 (1994) 71.
[38] R.K. Sharma, J.B. Wooten, V.L. Baliga, X. Lin, W.G. Chan, M.R. Hajaligol, Fuel 83 (2004) 1469.
[39] P.G. Hatcher, Energy Fuels 2 (1988) 48.
[40] H. Knicker, A. Hilscher, F.J. González-Vila, G. Almendros, Org. Geochem. 39 (2008) 935.
[41] P.G. Hatcher, E.C. Spiker, N.M. Szeverenyi, G.E. Maciel, Nature 305 (1983) 498.
[42] I. Kögel-Knabner, F. Ziegler, M. Riederer, W. Zech, Zeitschr. Pflanzenernähr. Bodenk 152 (1989) 409.
[43] G.A. lmendros, F.G. González-Vila, F. Martín, R. Fründ, H.D. Lüdemann, Sci. Total Environ. 117–118 (1992) 63.
[44] H. Knicher, G. Almendros, F.J. González-Vila, F. Martín, H.-D. Lüdemann, Soil Biol. Biochem. 28 (1996) 1053.
[45] H. Knicker, Biogeochemistry 85 (2007) 91.